11-2020

Chapter 1.1: 3-D Surface Visualization of pH Titration "Topos": Equivalence Point Cliffs, Dilution Ramps and Buffer Plateaus

Garon C. Smith
University of Montana, Missoula

Md Mainul Hossain
North South University, Bangladesh

Patrick MacCarthy
Colorado School of Mines

Part 1: Acid-Base Equilibrium

Chapter 1.1
3-D Surface Visualization of pH Titration "Topos": Equivalence Point Cliffs, Dilution Ramps and Buffer Plateaus

Garon C. Smith[1], Md Mainul Hossain[2] and Patrick MacCarthy[3]
[1]Department of Chemistry and Biochemistry, The University of Montana, Missoula, MT 59812, Department of Biochemistry and Microbiology, North South University, Dhaka, Bangladesh, and [2]Department of Chemistry and Geochemistry, Colorado School of Mines, Golden, CO 80401

Abstract

3-D topographic surfaces ("topos") can be generated to visualize how pH behaves during titration and dilution procedures. The surfaces are constructed by plotting computed pH values above a composition grid with the volume of base added in one direction and the overall system dilution on the other. What emerge are surficial features that correspond to pH behavior in aqueous solutions. Equivalence point breaks become cliffs that pinch out with dilution. Buffer effects become plateaus. Dilution alone generates 45° ramps. Limitations of the Henderson-Hasselbalch equation can be seen by noting the conditions over which a plateau remains relatively flat. Because dissociation is driven by dilution, the surfaces demonstrate the point at which the solution of a weak acid becomes indistinguishable from that of a strong acid. Surfaces are presented for hydrochloric acid, HCl (a strong acid); acetic acid, CH_3COOH (a weak monoprotic acid); oxalic acid, HOOCCOOH (a weak diprotic acid) and L-histidine dihydrochloride, $C_6H_9N_3O_2 \cdot 2HCl$ (a weak triprotic acid). Supplementary materials include pH TOPOS, the macro-enabled spreadsheets that quickly generate surfaces for any mono-, di- or triprotic acid desired. Only a change of acid dissociation constants, $\mathcal{K}_a$ values, is required. Also provided are a PowerPoint lecture for teaching pH topos in the classroom, practice/homework exercises, and laboratory activities for first-year college courses and junior- or graduate level analytical chemistry courses.

The pH topo surface for carbonic acid.

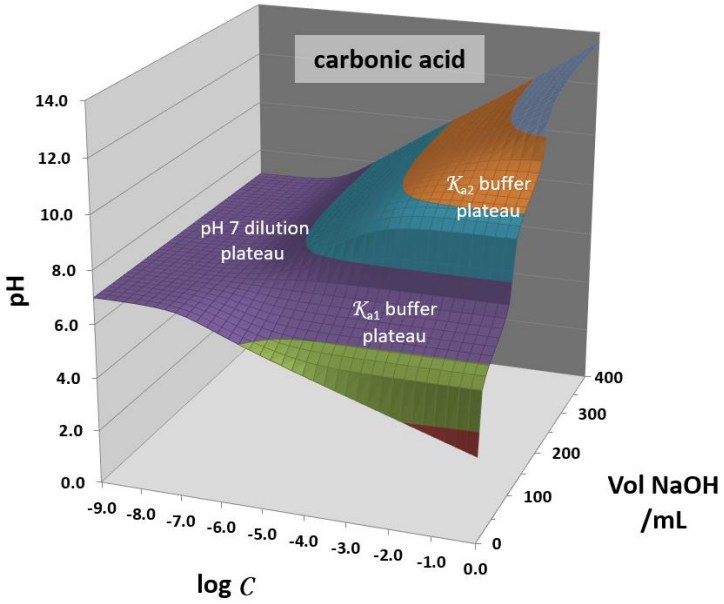

1.1.1 Introduction

One of the traditional approaches to understanding acid-base chemistry and pH is to study titration curves. Titration curves appear in virtually every general chemistry text[1-3] and titration procedures constitute an experiment in essentially every introductory laboratory manual.[4,5] But there are subtleties to titration curves that are often overlooked. For example, as a system is diluted, the magnitude of the equivalence point break deteriorates, buffer plateaus erode and auto-dissociation of water eventually begins to dominate a system. This paper introduces 3-D topographic pH surfaces (topos) with "cliffs", "plateaus" and "ramps" that change with addition of base or dilution of the system.

The pH topos are designed to help beginning students see how acid dissociation constants, their $\mathcal{K}_a$'s, affect pH and titration curves. As such, they are appropriate in teaching pH fundamentals in first-year college chemistry courses. But because the topos invite the reader to consider acid-base behavior over a broad range of conditions, they can also help students in upper-division and graduate analytical chemistry courses appreciate some nuances of acid-base behavior. Most specifically, the topos reveal how dilution affects a buffered system, a topic not pursued in standard analytical texts. The interactive spreadsheets permit students to quickly see the results of what would otherwise be an infeasible set of extensive calculations. Supplementary materials include suggested uses of pH topos in lecture, as worksheets and in support of laboratory activities.

1.1.2 Titration Curve Calculations

S.P.L. Sørensen first formulated the concept of pH in 1909[6], realizing that pH control via buffers was critical to his experiments with enzymes. But pH as a concept in introductory chemistry courses did not occur until about forty years later.[7] Even then, before the advent of digital computers, rigorous pH calculations were arduous. Titration curves were often computed using approximations with concomitant underlying assumptions. As computers and hand-held calculators evolved, a steady stream of papers appeared regarding how to solve the exact equations using numerical methods. A leader in this area was Lars Sillén of Sweden's Royal Institute of Technology.[8] Software packages that performed a wide variety of titration calculations for pH, buffers and species distributions were available from JCE Software in 1989[9] and in an updated version again in 1998.[10] Unfortunately, these are no longer available. At this writing, CurTiPot, spreadsheets that do many of the same functions, is provided as a free download from I.G.R. Gutz.[11] This paper introduces a 3-D topo surface approach to pH and buffer calculations that offers new insights into old topics. Included in the Supplementary Materials is an Excel workbook with embedded macros that will allow the reader to reproduce all pH surfaces discussed here as well as allowing them to create a pH surface for any other mono-, di- or triprotic acid they wish to view. The only inputs required are acid dissociation constants, $\mathcal{K}_a$ values.

Calculations utilized in creating the figures in this paper were performed in the Excel environment using its Visual Basic programming capabilities. For topo surface plots, pH values must be calculated at regularly spaced grid intervals. A grid point consists of the volume of base added plus the logarithm of the overall system dilution, ($\mathcal{V}_b$, log $\mathcal{C}$). The regular volume intervals required for topos demand numerical methods to solve a higher order polynomial expression for each grid point. Many titration curve calculations in the literature are done in the inverse direction where the pH is stepped at regular intervals and plotted at whatever volume of base results.[12, 13] While this approach offers computational ease, it is not suitable for topo surface plots. A separate gridding operation would be required to interpolate pH values to grid-point coordinates.

Grid point pH values were computed to 15 significant figures. This permits species concentrations to be expressed far beyond the precision that can be measured in real experimental procedures. While such precise results are beyond any instrumentation, they are completely valid in a theoretical sense. For the

purpose of clarity, activity effects have not been explicitly included in the model systems. Their inclusion would be necessary before modeled results would match experimental measurements. But they would not affect any of the conceptual points made in this chapter. Real systems, whose ionic strength is controlled, would exhibit surfaces identical to those in this paper except for scalar factors.

Values for $\mathcal{K}_a$s are taken from Martell and Smith's Critical Stability Constants.[14]

1.1.3 The Titration/Dilution pH Topo Surface

The discussion of pH changes and buffers is usually illustrated by means of titration curves. But a single titration curve displays only one set of experimental concentrations. As the reagents for a titration are diluted, the associated titration curve also changes (Figure 1.1-1). This point is made by many authors who, with multiple traces, show the equivalence point break diminishing as one goes to progressively more dilute conditions.[15-17] A close examination of the curves reveals that dilution causes each successive curve to start at a slightly higher pH level plus the magnitude of the post-equivalence point plateau drops by one pH-unit each time the reagents are diluted by a factor of 10.

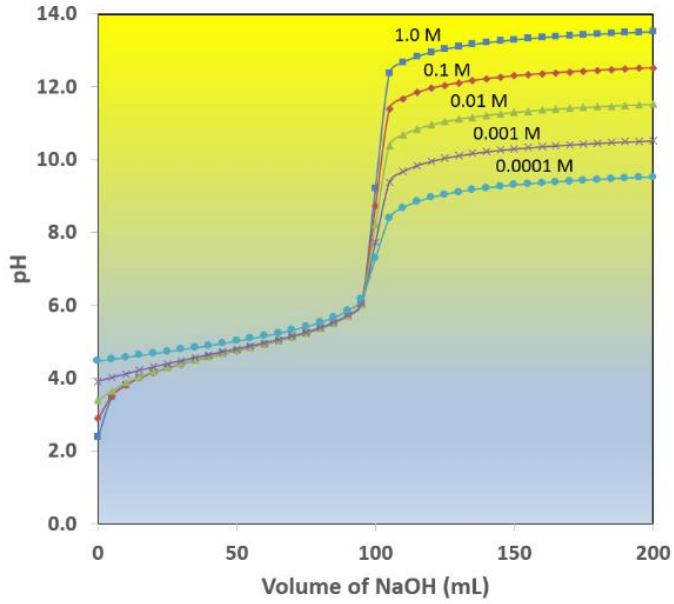

Figure 1.1-1. Dilution effects on a titration curve for 100 mL of acetic acid titrated with NaOH. Both the acetic acid and NaOH stock solutions are at the molarity noted on each trace.

A more comprehensive view of pH behavior during acid-base titrations can be visualized by plotting 3-D topo surfaces above a composition grid that encompasses a wide range of reagent concentrations. The grid is constructed by recording the progress of a titration (volume of strong base added) on the x-axis and following the overall dilution of the system (log C) on the y-axis. All concentrations are expressed in molarity (M). It is important to note that the x-axis is linear while the y-axis is logarithmic. When the pH associated with a set of regularly spaced grid points is plotted on the logarithmic z-axis, a 3-D pH topo surface is generated. All surfaces for this paper are based on an initial volume of 100.0 mL for the acid analyte.

The pH topo surface for acetic acid is shown in Figure 1.1-2 based on a K_a of 1.75 x 10^{-5}. The right-hand edge of the surface corresponds to a traditional titration curve as seen in texts and papers. As one moves to the left along the log C axis, progressively more dilute conditions are encountered. For the most concentrated system (*i.e.*, the line that forms the right-hand edge of the surface), 1.0 M CH_3COOH is being titrated with 1.0 M NaOH. Successive lines in the dilution direction indicate repeating the titration with both the acid and base concentrations adjusted identically. Thus, at the most dilute point (the left-hand edge of the surface), 1.0 x 10^{-9} M CH_3COOH is being titrated with 1.0 x 10^{-9} M NaOH. The five traces in Figure 1.1-1 are simply five of the 37 slices that comprise the overall pH topo of Figure 1.1-2, specifically, those slices that correspond to the log C values of 0, -1, -2, -3, and -4. On the complete topo surface, finer gradations between whole-numbered dilution values are seen.

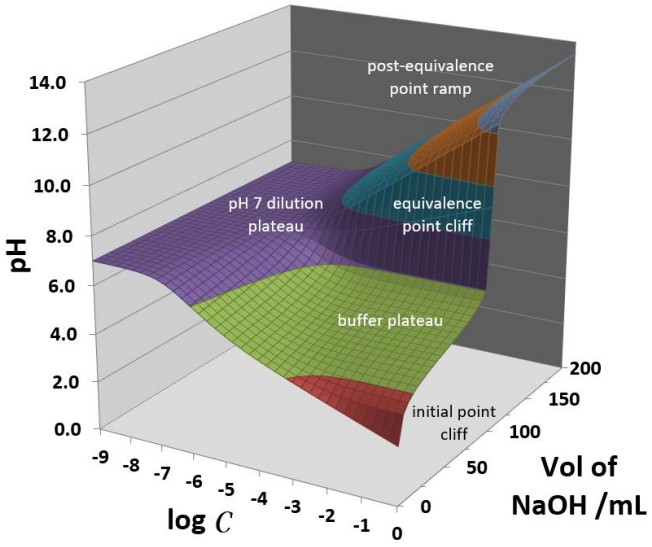

Figure 1.1-2 The acetic acid pH topo surface for a 100 mL sample.

With an entire pH topo surface to view, one can discern a series of ramp, cliff and plateau features. Ramps are associated with grid regions where dilution dominates the solution's pH. Cliffs occur at initial and equivalence points during a titration procedure. Plateaus are indicative of situations in which pH is somewhat stable, *i.e.*, buffer zones or extreme dilution conditions.

The equivalence point cliff on the acetic acid pH topo appears at 100 mL of NaOH added. At the equivalence point, the solution is identical to dissolving pure $NaCH_3COO$ in water. Beyond the 100 mL mark, excess NaOH titrant is now being added to the solution. Because NaOH is a strong base, the pH rapidly rises toward the pH of the titrant solution itself.

As one moves to the left on the topo surface with dilution, the heights of cliffs diminish and all ramps proceed toward a pH 7 dilution plateau. Notice, for example, the change in the equivalence point cliff from its dramatic rise at a log C of 0 to its pinched out ending at a log C of about -6. As titration traces to the left are considered, the concentration of the NaOH titrant (as well as that of the analyte) is being systematically lowered. For a while, each log unit moved to the left also drops the post-equivalence point ramp pH by one unit. Eventually, however, when the titrant becomes sufficiently dilute with respect to NaOH (*e.g.*, 1.00×10^{-6} M), the contribution of OH^- from auto-dissociation of water (1×10^{-7} M) begins to become more significant. By the last titration slice, when the titrant is 1.0×10^{-9} M NaOH, the OH^- from water overwhelms that from the titrant a hundred-fold. The concentration of OH^- in the 10^{-9} titrant would actually be 1.01×10^{-7} M where the first "1" is OH^- from water and the second "1" is OH^- from NaOH. The pH of this titrant is essentially 7. So, too, the pH of the starting analyte mixture is about 7. From modeling calculations, the H_3O^+ concentration in 1×10^{-9} M CH_3COOH at the start is 0.000 000 100 498 M, a pH of 6.9978. There is no equivalence point cliff in the pH 7 dilution plateau because the total pH range of the entire trace only varies from 6.9978 at 0.0 mL NaOH added to 7.00073 at 200.0 mL of NaOH added.

1.1.4 Strong Acid vs. Weak Acid Topo Surfaces

To better understand the initial point cliff and buffer plateau features on the acetic acid pH topo surface of Figure 1.1-2, it is helpful to first look at the topo

for a strong acid-strong base titration. An example of this, the pH topo surface for hydrochloric acid titrated with NaOH, is shown as Figure 1.1-3.

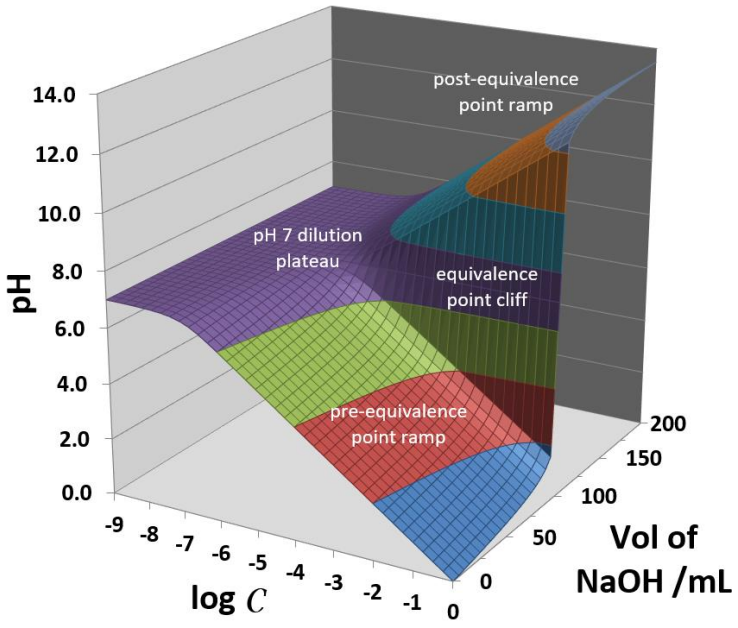

Figure 1.1-3. The hydrochloric acid pH topo for a 100 mL sample

The pH topo for a strong acid shows no plateau in front of the equivalence point cliff. There is simply a broad pre-equivalence point ramp. This ramp shows solution behavior when there are no buffer interactions occurring. In the volume direction, the pH shows a shallow rise until the equivalence point is reached. This is "pseudo-buffering", an artifact of the logarithmic nature of pH.[18] With dilution, however, there is a direct relationship with pH. The pre-equivalence point ramp rises to the left at a 45° slope; the concentration of H_3O^+ changes by an order of magnitude with each order of magnitude change caused by dilution. The linearity of the ramp eventually begins to degrade as contributions of H_3O^+ from the water of dilution start to become significant at about a log C of -6.

Weak acid pH topo surfaces will have a buffer plateau and an initial point cliff that is not seen with a strong acid pH surface. This is immediately apparent when comparing Figures 1.1-2 and 1.1-3. To assist in visual comparison, Figure 1.1-4 superimposes the pH topo of acetic acid on top of that for HCl. The influence of the buffer action between acetic acid and acetate ion lifts the pH surface above the pre-equivalence point ramp. Any portions of the pH surface that are oriented at less than a 45° angle in the dilution direction have some buffer influence taking place.

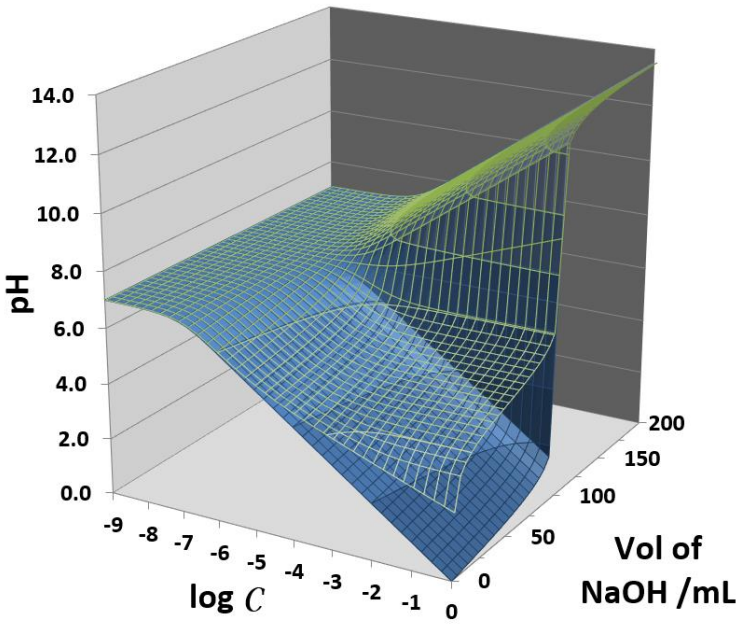

Figure 1.1-4. Overlay of pH topo surfaces for acetic acid (upper) and hydrochloric acid (lower).

1.1.5 A Detailed Analysis of Other Topo Features for Acetic Acid

Weak acids will usually exhibit both an initial point cliff as well as a buffer plateau prior to the equivalence point cliff. Acetic acid is a typical monoprotic carboxylic acid. Its buffer plateau is centered around pH = p$\mathcal{K}_a$ = 4.757 and extends from the front edge of the surface to about midway toward the back. In the volume direction, it sits between the initial point cliff and the equivalence point cliff. This is the type of buffer behavior that is generally described. Most introductory chemistry texts introduce the Henderson-Hasselbalch equation[19] to demonstrate that pH is primarily governed by the p$\mathcal{K}_a$ and is then modified by the ratio of the buffer's base form to acid form to account for any imbalance in their relative amounts (Eq 1.1-1).

$$\text{pH} \cong \text{p}\mathcal{K}_\text{a} + \log\frac{C_\text{b}}{C_\text{a}} \qquad (1.1\text{-}1)$$

C_b and C_a are the respective stoichiometric concentrations of the base and acid forms of the buffer compound uncorrected for dissociation and hydrolysis. This is really just a special case for the more general Mass Action Law of Guldberg and Waage.[20, 21] The Henderson-Hasselbalch form is only valid at relatively high concentrations of acid and base, C_a and C_b. Movement along the volume axis

corresponds to adding a relatively concentrated solution of strong base, NaOH. When the base buffer capacity is exceeded, the Henderson-Hasselbalch equation no longer holds. The pH rapidly shoots upward at the equivalence point cliff, headed eventually for the pH of the NaOH solution that is being used as the titrant.

Less frequently discussed is buffer behavior of a system as it undergoes dilution. A classical treatment of this subject was presented by Bates in 1954.[15] He organized his discussion around the pH shift caused by diluting a sample by a factor of two, $\Delta pH_{1/2}$, and follows dilution effects over a total dilution range of 40-fold. The treatment in this paper tracks the pH changes through a much larger dilution range – nine orders of dilution magnitude.

Dilution of a buffer is a complex situation. For this analysis, it is better to consider the logarithmic form of the Guldberg and Waage Mass Action Law (Eq 1.1-2) that is general for all conditions. [20, 21] Note that, unlike Eq 1.1-1, it employs equilibrium concentrations rather than stoichiometric concentrations.

$$pH = p\mathcal{K}_a + \log\frac{\left[CH_3COO^-\right]}{\left[CH_3COOH\right]} \qquad (1.1\text{-}2)$$

When the pH of the buffer plateau is less than 7, the dilution effects are largely controlled by the concentration of the buffer's acid form. Diluting a 1.0 M H_3O^+ solution by ten, for instance, should drop the H_3O^+ concentration to 0.1 M and give rise to an ~1 pH unit change. This is where changes would stop with concentrated solutions of a strong acid and is the basis for the pre-equivalence point ramp for the HCl surface in Figure 1.1-3. But a solution containing a buffer will rebound from the dilution-caused pH rise. The basis for the counteraction comes out of the acid dissociation reaction (Eq 1.1-3).

$$CH_3COOH + H_2O \rightleftharpoons CH_3COO^- + H_3O^+ \qquad (1.1\text{-}3)$$

Because H_2O is a reactant in Eq 1.1-3, Le Chatelier's principle/mass action law dictates that the reaction will shift to the right until a new equilibrium is established. Thus, $[CH_3COOH]$ will drop and $[CH_3COO^-]$ will rise. If the buffer is working well, the system will rebound to almost the same pH as before the dilution occurred. The dissociation of CH_3COOH needs to supply essentially 90% of the H_3O^+ if the effect of 10-fold dilution is to be overcome. Dilution will also

drive the base form's hydrolysis reaction, but this will be negligibly small in magnitude because $\mathcal{K}_a$ (1.75 x 10^{-5}) >> $\mathcal{K}_b$ (5.71 x 10^{-10}).

Consider the situation at the half-equivalence point volume of 50 mL of NaOH added (the Before Dilution line in Table 1.1-1 below). Next, let the system be diluted by a factor of ten (the After Dilution line in Table 1.1-1). This has upset an equilibrium that will now shift toward the right in Eq 1.1-3 until an equilibrium has once again been established. Using the $\mathcal{K}_a$ for acetic acid and the starting values in the After Dilution line, one can solve for the amount of the shift. This is calculated to be 1.573 x 10^{-5} M which can be used to correct the After Dilution values to the new At Equilibrium values. These reveal that acetic acid has dissociated a small amount, but this amount of dissociation provides enough H_3O^+ to almost make up for the 10-fold dilution factor. Instead of the pH rising by one whole pH unit as dilution would suggest, the new pH has only risen 0.00041 pH units from its Before Dilution value.

Table 1.1-1. A dilution example for a 1.0 M system of acetic acid.

	$[H_3O^+]$	$[CH_3COO^-]$	$[CH_3COOH]$	base/acid ratio	pH
Before dilution	1.749816 x 10^{-5}	0.3333508	0.3333158	1.000105	4.7570075
After dilution*	1.839816 x 10^{-6}	0.03333508	0.03333158	1.000105	5.7535226
At equilibrium	1.748165 x 10^{-5}	0.03335081	0.03331585	1.001049	4.7574175

*Includes a contribution of $[H_3O^+]$ from the pH 7 diluent water before accounting for equilibrium shifts

As long as there is a sufficient quantity of the acid form to dissociate, it maintains a reservoir of stored protons ready to be released through dissociation. The Henderson-Hasselbalch equation is valid for dilution events as long as only a small part of the acid form must dissociate. Note in Table 1.1-1 that the ratio of base form to acid form has only changed by about 0.1% between the Before and After dilution values.

With successive 10-fold dilutions, an increasing proportion of the acid form must dissociate to maintain the pH. Consider, for example, a 10-fold dilution when the system concentration is 1.0 x 10^{-3} M. Table 1.1-2 demonstrates that a higher percentage of the acid form disappears. This results in a noticeable change in the base/acid ratio. Eq 1.1-2 shows that as the base/acid ratio changes, so too does the pH. The ~65% shift in the ratio translates into a pH rise of 0.2172279 pH units. Note that the concentration of acetic acid drops by more than an order of magnitude. One order of magnitude for the drop is lost because of dilution. It drops even more, though, because now significant amounts of CH_3COOH are

being converted to the base form through dissociation caused by H_2O driving Eq 1.1-3 even further to the right. It is ~34% lower than just dilution would cause. Conversely, the concentration of acetate does not drop by an order of magnitude, but is 23% higher than dilution alone would produce.

Table 1.1-2 A dilution example for a 10^{-3} M system of acetic acid in which the Henderson-Hasselbalch equation is beginning to fail.

	$[H_3O^+]$	$[CH_3COO^-]$	$[CH_3COOH]$	base/acid ratio	pH
Before dilution	1.590600×10^{-5}	3.492387×10^{-4}	3.174280×10^{-4}	1.100214	4.7984391
After dilution*	1.680600×10^{-6}	3.492387×10^{-5}	3.174280×10^{-5}	1.100214	5.7745356
At equilibrium	9.645684×10^{-6}	4.297798×10^{-5}	2.368869×10^{-5}	1.814283	5.0156670

*Includes a contribution of $[H_3O^+]$ from the pH 7 diluent water before accounting for equilibrium shifts

As the dilution of a system approaches 10^{-6} M, a new controlling force for the system pH begins to emerge, namely the H_3O^+ and OH^- content of the diluent water where $[H_3O^+]$ and $[OH^-]$ are both 1.0×10^{-7} M. Continued additions of this level of H_3O^+ and OH^- begin to overtake influences from the small quantities of buffer components that are present. Table 1.1-3 illustrates details of this situation at 10^{-7} M. The diluent water has nearly the same $[H_3O^+]$ as the Before Dilution system, so the After Dilution concentration changes little. CH_3COOH is still undergoing further dissociation with dilution, but the H_3O^+ it produces (6.06685×10^{-12} M) contributes little. The overall system's $[H_3O^+]$ is nearly five orders of magnitude larger at 1.016610×10^{-7} M. The upward drift essentially stops when the titration surface pH reaches the vicinity of 7. It is interesting to note, however, that the base to acid ratio continues to change as required by mass action effects.

Table 1.1-3. A dilution example for a 10^{-7} M system of acetic acid in which contributions from the auto-dissociation of H_2O become significant.

	$[H_3O^+]$	$[CH_3COO^-]$	$[CH_3COOH]$	base/acid ratio	pH
Before dilution	1.177868×10^{-7}	6.622096×10^{-8}	4.457116×10^{-10}	148.5735	6.9289034
After dilution*	1.017787×10^{-7}	6.622096×10^{-9}	4.457116×10^{-11}	148.5735	6.9579056
At equilibrium	1.016610×10^{-7}	6.628162×10^{-9}	3.850431×10^{-11}	172.1408	6.9928457

*Includes a contribution of $[H_3O^+]$ from the pH 7 diluent water before accounting for equilibrium shifts

1.1.6 The Effect of p$\mathcal{K}_a$ on pH Changes Caused by Dilution

The lower the p$\mathcal{K}_a$, the sooner dilution causes the buffer plateau to start drifting upwards. Figure 1.1-5 illustrates modeled systems for weak acids with hypothetical p$\mathcal{K}_a$s of 1, 2, 3, etc. The traces shown are the dilution slices at 20 mL of NaOH added, a volume that will display any buffer plateaus that exist. Also included is a trace for the 20-mL slice of HCl so that visual comparisons with a strong acid can be made.

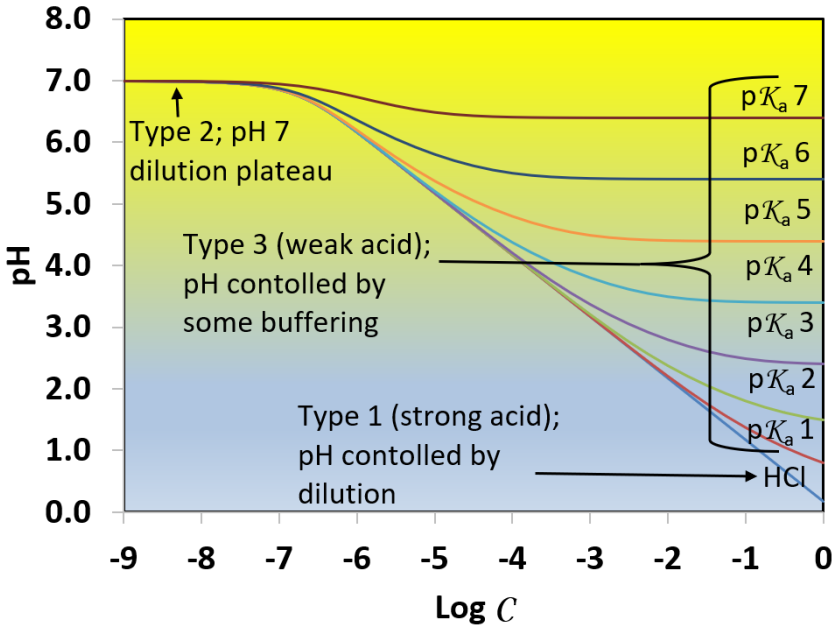

Figure 1.1-5. Dilution effects on pH vs. p$\mathcal{K}_a$ value for 20 mL-added slices.

There are three possible pH behaviors that can occur upon dilution:

Type 1) the pH can vary directly with the amount of dilution;

Type 2) the pH can be controlled by the auto-dissociation of the diluent water:

Type 3) the pH can be stabilized to varying extents by the presence of a buffer system

A strong acid system exhibits behaviors 1 and 2 only while a weak acid system may exhibit all three (Figure 1.1-5). As soon as the weak acid trace begins to overlap the HCl trace, strong and weak acids exhibit the same Type 1 dilution behavior.

A strong acid system shows no buffer character with dilution. Strong acids essentially dissociate completely, so essentially no associated form, *i.e.*, an HCl

molecule, exists in water to react with added OH^-. The only significant acid in the system is H_3O^+. As a concentrated system is diluted, so too is the H_3O^+. This is the Type 1 behavior listed above and leads to a graphical trace that rises at a 45° angle to the left. Eventually, however, the H_3O^+ content of the diluent water itself becomes significant compared to the diluted H_3O^+ produced by the strong acid. When the system approaches 10^{-6} M, the H_3O^+ from diluent water starts to make headway over the remaining trace-level amounts of strong acid. Ultimately, it completely overwhelms the original H_3O^+ from the strong acid. The pH sits close to 7, the pH of pure water. This is Type 2 behavior.

A weak acid system will demonstrate Type 3 behavior, a situation in which the effect of dilution is counteracted, sometimes almost completely. This is buffering against dilution and will occur to greater and greater extents as the pK_a of the acid approaches 7.00 (Figure 1.1-5). Weak acids only partially dissociate upon dilution, but they release sufficient protons in doing so that the pH does not rise so swiftly. The reason that pK_as closer to 7.00 show more protracted buffering against dilution is because: the weaker the acid, the less it dissociates when placed in water. Ever greater degrees of dilution are required to consume its base buffer capacity. Figure 1.1-6 illustrates how many orders of magnitude of dilution are required to raise the pH of the system by 1 unit at the half-equivalence point. This is illustrative of where the assumptions in the Henderson-Hasselbalch equation (Eq1.1-1) are beginning to fail. By the time the pH has risen one unit, 90.9% of the acid form has been consumed. Note that $pK_a = 5$ is the highest value shown in Figure 1.1-6. With a pK_a of 6, there is never a 1-pH unit rise caused by dilution.

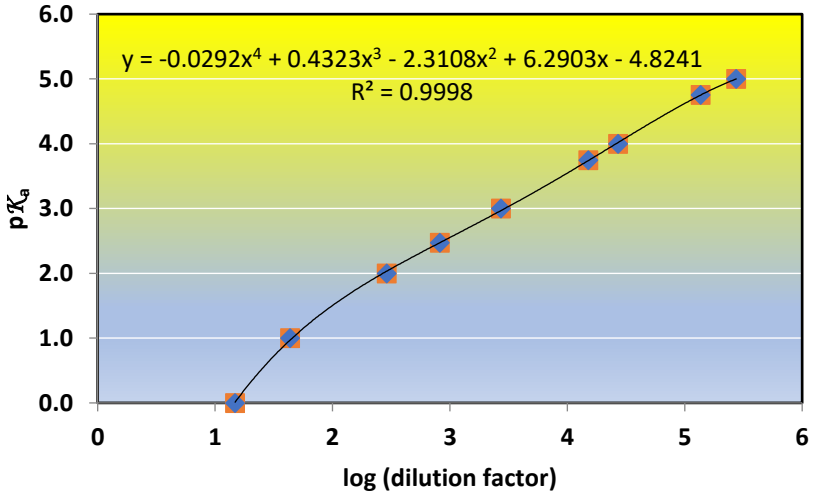

Figure 1.1-6. Orders of magnitude of dilution required to shift the base form/acid form ratio by a factor of 10 at the half equivalence point.

Eventually, weak acids with p$\mathcal{K}_a$s lower than 7 dissociate to the point at which they are indistinguishable from a strong acid. Figure 1.1-5 illustrates this point for weak acids. At a log $\mathcal{C}$ around -6.0, there is no difference between the acidity of a solution of HCl and a weak acid with a p$\mathcal{K}_a$ of 5. Under these conditions, the p$\mathcal{K}_a$ 5 weak acid acts like a strong acid, *i.e.*, 100% dissociated.

As a special case, consider a hypothetical acid with a p$\mathcal{K}_a$ of 7.00. This acid would exhibit perfect buffering against dilution to any extent. Our modeled system for the p$\mathcal{K}_a$ 7.00 acid shows a dilution slice at the 50-mL half-equivalence point with a pH of exactly 7.00000… across the entire surface. The species distribution coefficients, α_0 (the fraction of acetic acid in the protonated form) and α_1 (the fraction of acetic acid in the deprotonated form), are uniformly 0.500000… across the entire surface as well. This is consistent with the Mass Action law (Eq1.1-2 above). At pH=7.00, the ratio of base form to acid form is always 1.00000…., so the log term disappears. Dilution does not affect the pH.

1.1.7 pH Topo Surfaces for Polyprotic Acid Titrations

The pH topo surfaces for polyprotic acids have the same types of features – cliffs, plateaus and ramps – just more of them. Figure 1.1-7, for example, displays the pH topo surface for the diprotic oxalic acid. The modeled surface is based on a $\mathcal{K}_{a1}$ of 5.6 x 10^{-2} (p$\mathcal{K}_{a1}$ =1.252) and a $\mathcal{K}_{a2}$ of 5.42 x 10^{-5} (p$\mathcal{K}_{a2}$ of 4.266). The first $\mathcal{K}_a$ is so low that oxalic acid is already missing most of its first titratable proton when initially dissolved in water. This leads to no initial point cliff being observed as it was for acetic acid. Note that there are two equivalence point cliffs, one for each of the two protons that can react with NaOH. Unless successive p$\mathcal{K}_a$s are well separated, the equivalence point breaks are small. Thus, the first equivalence point cliff for oxalic acid is not dramatic because the difference between p$\mathcal{K}_{a1}$ and p$\mathcal{K}_{a2}$ is only 3.14. The first equivalence point cliff begins pinch out at about log $\mathcal{C}$ = -2.

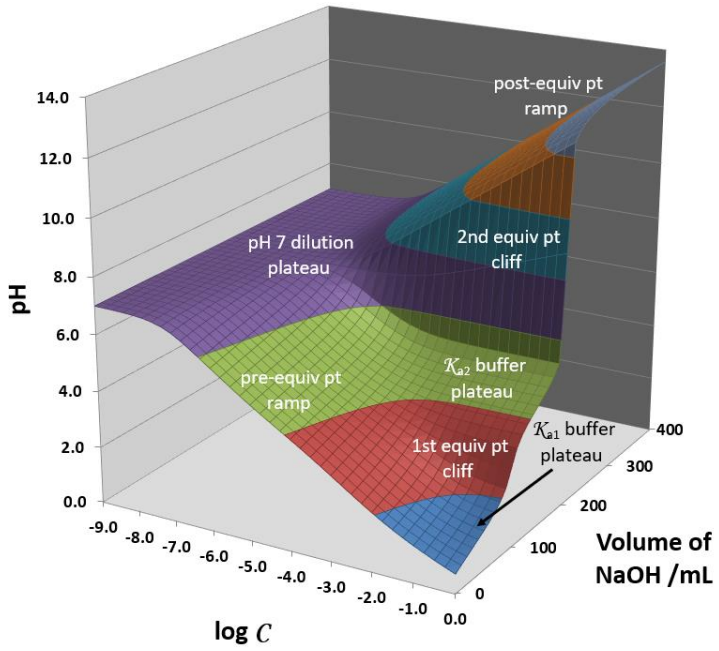

Figure 1.1-7. The pH surface for diprotic oxalic acid (HOOCCOOH)

Recall that the extent of buffer plateaus is related to the p$\mathcal{K}_a$ of the acid form. Because the p$\mathcal{K}_{a1}$ for oxalic acid is so low, its ability to buffer against dilution has essentially already been exceeded by simply dissolving it in water (see p$\mathcal{K}_a$ = 1 trace in Figure 1.1-5). The buffer plateau associated with the p$\mathcal{K}_{a2}$ of 4.266 extends to about log C_{dil} = -5, as predicted from Figure 1.1-6.

While oxalic acid can be modeled at a concentration of 1.0 M, in reality, a saturated solution in water at 25°C is about 0.1 M. Thus, in experimental settings, the first equivalence point break will always be small. The second equivalence point break extends all the way to the pH 7 dilution plateau. This happens for any system for which the p$\mathcal{K}_{a2}$ associated with the break is within the range of 4 - 7.

An example of the triprotic pH topo surface for L-histidine dihydrochloride (H_3his^{2+}) is presented in Figure 1.1-8. The $\mathcal{K}_a$s used in its calculation were 3 x 10^{-2}, 1.07 x 10^{-6} and 5.2 x 10^{-10} (or p$\mathcal{K}_a$s of 1.6, 5.97 and 9.28, respectively). It shares similar features to the oxalic acid topo surface up to the second equivalence point break. It has no initial point cliff and essentially no buffer plateau for the first proton. The first equivalence point break is more pronounced than that of oxalic acid because the difference in p$\mathcal{K}_{a1}$ and p$\mathcal{K}_{a2}$ is 4.37, more than one unit larger. The only new feature seen with the L-histidine dihydrochloride surface is a third

equivalence point above pH 7. The third buffer plateau (pH = p$\mathcal{K}_{a3}$ = 9.28) begins to degrade before the -3 level on the log $\mathcal{C}$ axis. In this instance, $\mathcal{K}_{b1}$ >>$\mathcal{K}_{a3}$ so the diluent water is driving the hydrolysis reaction to re-protonate the his$^-$ species. From log $\mathcal{C}$ values of -3 to -7, mass action effects from diluent water drive the protonation of his$^-$ and converts it to Hhis. At these alkaline starting pHs, very little H_2his^+ is present to dissociate in opposition. From alpha species distribution calculations, the pH 7 dilution plateau shows a mixture that is roughly 90% Hhis and 10% H_2his^+.

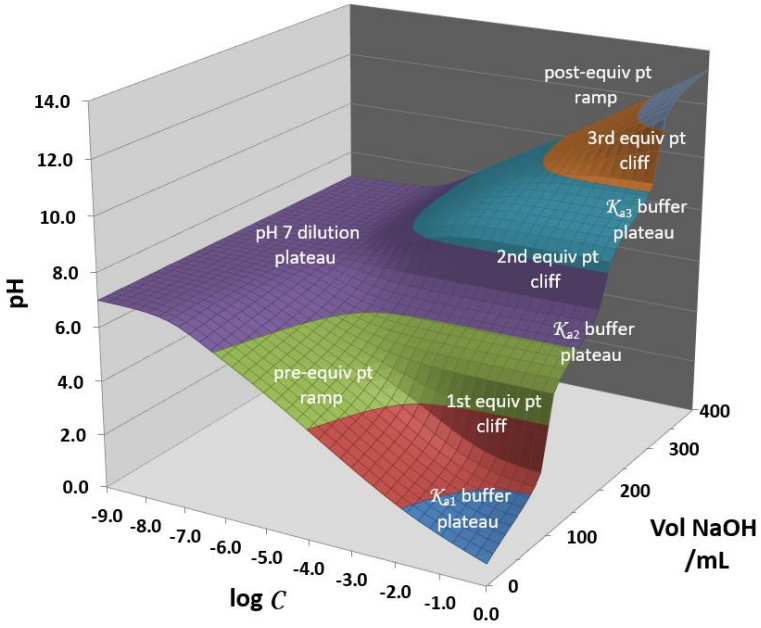

Figure 1.1-8. The pH surface for triprotic L-histidine dihydrochloride ($C_6H_9N_3O_2 \cdot 2HCl$)

The pH TOPO software permits one to easily illustrate conditions under which equivalence point breaks will be weak or unseen. This can happen whenever: Case 1) successive p$\mathcal{K}_a$s are spaced at less than three orders of magnitude; Case 2) a p$\mathcal{K}_a$ is not at least three units higher than the pH of the initial solution; or Case 3) when a p$\mathcal{K}_a$ is not a least three units lower than the pH of the titrant base. Citric acid illustrates Case 1 as seen in Figure 1.1-9, Panel a. Because it is a triprotic acid, it has three equivalence points. Its three p$\mathcal{K}_a$s of 3.128, 4.761 and 6.396, however, are spaced at intervals less than 3. Only the 3rd equivalence point cliff is visible as a topo cliff. Here, the p$\mathcal{K}_{a3}$ (6.396) and the pH of the titrant (14.000) do differ by more than 3. A good example of Case 2 occurs with sulfuric acid (Figure 1.1-9, Panel b). Sulfuric acid's first proton is strong with a p$\mathcal{K}_a$ of -6, well below the initial pH of -0.004. A barely visible warp in the topo surface can be discerned at the first equivalence point volume of 100 mL. The small warp is evidence that the second proton is a weak acid proton. Case 3 is

seen with the phosphoric acid surface. Its 3rd equivalence point is barely visible. There is only a difference between its p$\mathcal{K}_{a3}$ of 12.375 and the pH 14 for the titrant of 2.625.

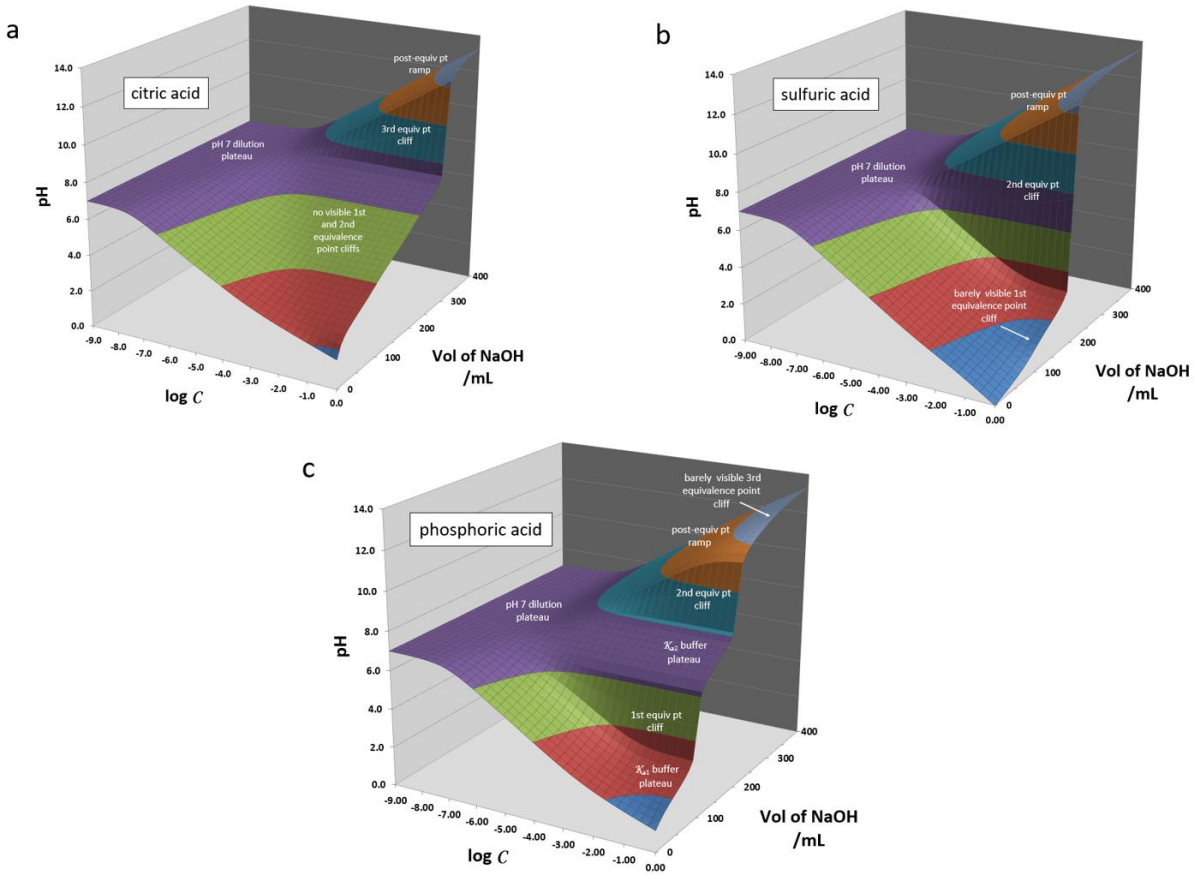

Figure 1.1-9. Topos illustrating weak or not visible equivalence point cliffs. a) Case 1 - p$\mathcal{K}_a$s too closely spaced; b) Case 2 - p$\mathcal{K}_a$ not at least 3 units higher than initial pH; c) Case 3 - p$\mathcal{K}_a$ not at least 3 units lower than titrant pH.

1.1.8 Conclusions

A 3-D visualization of pH topo surfaces on the titration/dilution composition grid helps draw out subtle aspects of acid-base chemistry that might otherwise be overlooked. It converts a myriad of tedious calculations into a single, easy to understand picture. Students are much more likely to grasp difficult concepts from an image than they are from an abstract equation. This is especially true with regard to how dilution influences the pH of a system. The

software provided in the macro-enabled Excel worksheets makes it possible for students to EASILY view pH topo surfaces for a multitude of acids. All a user needs to supply are $\mathcal{K}_a$ values, many of which are tabulated within a program worksheet. About 20 seconds later, a complete pH topo surface is displayed. For advanced students, data for $[H_3O^+]$ and the associated pH values for every grid point can be examined in detail.

A particularly nice outcome of the pH surface approach is a visual demonstration of the limitations for the Henderson-Hasselbalch equation. The boundaries of the plateau portions of the surfaces denote where assumptions in the classical equation are breaking down. By noting that buffer plateaus persist with dilution to an extent that is a function of their p$\mathcal{K}_a$s is not a result that is easily seen in just looking at the equation itself.

All surfaces for this paper were modeled assuming that the diluent was pure water at pH 7.0. In reality, obtaining and maintaining a reservoir of water at pH 7.0 is extremely difficult unless you isolate the system in a CO_2-free atmosphere. Many of the points raised here would need to be modified if one used a typical surface water at pH 8.0 as the diluent or meteoric rainwater at pH 6.0. But with an understanding of the trends illuminated here, reasonable predictions of the changes would be rather straight forward.

We hope that the pH TOPOS program begins to replace the JCE titration curve software that is no longer available.

Acknowledgements

The authors are grateful to the Department of Chemistry and Biochemistry at The University of Montana for financial support of a graduate teaching assistantship during the course of these studies.

References

1. Cracolice, M.S.; Peters, E.I., *General Chemistry: An Inquiry Approach, Part II*, Cengage Learning, Mason, OH, 2013, Lesson 60 (How are the Concentrations of Acid and Base Solutions Determined?), 16p.
2. Chang, R.; Goldsby, K.A., *Chemistry,* 11 ed., McGraw-Hill, Columbus, OH, 2013, Chapter 16 (Acid-Base Equilibria and Solubility Equilibria).
3. Brown, T.E.; LeMay, H.E.H.; Bursten, B.E.; Murphy, C.; Woodward, P.; *Chemistry: The Central Science,* 12 ed., Pearson Prentice Hall, Upper Saddle River, NJ, 2013, Chapter 16 (Acid-Base Equilibria).

4. Abraham, M.R.; Pavelich, M.J *Inquiries into Chemistry,* 3 ed., Waveland Press, Long Grove, IL, 1999, Experiment G-2 (Acid and Base Interactions), 107-113.
5. Nelson, J.H.; Kemp, K.C.; Stoltzfus, M.W. *Chemistry: The Central Science, Laboratory Experiments,* 10 ed., Pearson Prentice Hall, Upper Saddle River, NJ, 2006.
6. Sørensen, S.P.L. Études enzymatiques. II. Sur la mesure et l'importance de la concentration des ions hydrogène dans les réactions enzymatiques, *Compt. rend. du Lab. de Carlsberg.* **1909**, *8*, 1–168.
7. Myers, R.J. One-Hundred Years of pH*, J. Chem. Educ.* **2010**, *87*(*1*), 30-32. https://doi.org/10.1021/ed800002c
8. Sillén, L.G. High-speed Computers as a supplement to Graphical Methods, *Acta Chem. Scand.* **1962**, *16* (*1*), 159-172. https://doi.org/10.1016/0039-9140(67)80203-0
9. Ramette, R.W. The Acid-Base Package: A Collection of Useful Programs for Proton Transfer Systems, *J. Chem. Educ. Software,* **1989**, *2B* No. 2.
10. Ramette, R.W. Buffers Plus, *J. Chem. Educ.* **1998**, *75*(11), 1504. https://doi.org/10.1021/ed075p1504
11. Gutz. I.G.R. http://www2.iq.usp.br/docente/gutz/Curtipot.html (accessed 10/23/20).
12. Waser, J. Acid-base titration and distribution curves*, J. Chem. Educ.* **1967***, 44,* 274-276. https://pubs.acs.org/doi/10.1021/ed044p274
13. *de Levie*, R. Explicit expressions of the general form of the titration curve in terms of concentration, *J. Chem. Educ.*, **1993**,70 (*3*), 209-217. https://pubs.acs.org/doi/abs/10.1021/ed070p209
14. Martell, A.E.; Smith, R.M. *Critical Stability Constants*, Plenum Press, New York, 1974.
15. Bates, R.G. Measurement of Effect of Dilution upon pH, *Anal. Chem*. **1954**, *26* (*5*), 871-874. https://pubs.acs.org/doi/abs/10.1021/ac60089a018
16. Christian, G.D. *Analytical Chemistry, 2nd ed.,* John Wiley, New York, 1977, p.231.
17. Harris, D. *Quantitative Chemical Analysis*, 8 ed., W.H. Freeman, New York, NY, 2011.
18. Clark, R.W., White, G.D., Bonicamp, J.M., Watts, E.D. From Titration Data to Buffer Capacities: A Computer Experiment for the Chemistry Lab or Lecture. *J. Chem. Educ*. **1995,** *72*(*8*), 746-750. https://doi.org/10.1021/ed072p746

19. Hasselbalch, K. A. Die Berechnung der Wasserstoffzahl des Blutes aus der freien und gebundenen Kohlensäure desselben, und die Sauerstoffbindung des Blutes als Funktion der Wasserstoffzahl, *Biochemische Zeitschrift* **1917,** *78*, 112–144.
20. Guldberg, C.M.; Waage, P. Über Die Chemische Affinität, *L. prakt Chem.* **1879**, *19*(2), 69-114.
21. de Levie, R. The Henderson approximation and the mass action law of Guldberg and Waage, *Chem. Educator* **2002**, *7*, 132-135. https://doi.org/10.1007/s00897020562a